

## Mode I Toughening Of Bio-based Epoxy Adhesive Through 3d-printed Biomimetic Reinforcements

Tao, R.; Xu, Z.; Teixeira De Freitas, S.

**Publication date**

2024

**Document Version**

Final published version

**Published in**

Proceedings of the 21st European Conference on Composite Materials

**Citation (APA)**

Tao, R., Xu, Z., & Teixeira De Freitas, S. (2024). Mode I Toughening Of Bio-based Epoxy Adhesive Through 3d-printed Biomimetic Reinforcements. In C. Binetruy, & F. Jacquemin (Eds.), *Proceedings of the 21st European Conference on Composite Materials: Volume 8 - Special Sessions* (Vol. 8, pp. 1321-1326). The European Society for Composite Materials (ESCM) and the Ecole Centrale de Nantes..

**Important note**

To cite this publication, please use the final published version (if applicable). Please check the document version above.

**Copyright**

Other than for strictly personal use, it is not permitted to download, forward or distribute the text or part of it, without the consent of the author(s) and/or copyright holder(s), unless the work is under an open content license such as Creative Commons.

**Takedown policy**

Please contact us and provide details if you believe this document breaches copyrights. We will remove access to the work immediately and investigate your claim.

# MODE I TOUGHENING OF BIO-BASED EPOXY ADHESIVE THROUGH 3D-PRINTED BIOMIMETIC REINFORCEMENTS

R. Tao<sup>1</sup>, Z. Xu<sup>1</sup> and S. Teixeira de Freitas<sup>1,2</sup>

<sup>1</sup>Aerospace Structures & Materials, Faculty of Aerospace Engineering, Delft University of Technology, Delft, the Netherlands

Email: R.Tao@tudelft.nl, Z.Xu-8@tudelft.nl

<sup>2</sup>IDMEC, Instituto Superior Técnico, Lisbon, Portugal

Email: Sofia.Teixeira.Freitas@tecnico.ulisboa.pt

**Keywords:** biomimetic, bio-based epoxy, 3D printing, adhesive joint, toughness

## Abstract

Bio-based epoxy materials face major challenges in their relatively poor mechanical properties compared to their petroleum-based competitors, including low fracture toughness and abrupt failure. By mimicking the molecular structure of spider silk, which is one of the toughest materials in nature, we manufactured polymer overlapping curls consisting of coiling fibers with sacrificial bonds and hidden lengths through 3D printing. These curls were embedded in a bio-based epoxy aiming to improve its toughness. The bio-based epoxy adhesive layer integrated by such 3D-printed coiling fibers was tested under mode I opening load using Double Cantilever Beam tests. The results show an extrinsic bridging triggered by the embedded curls that promote progressive failure and improve the mode I fracture toughness by 285%. The proposed 3D-printed coiling fibers can improve the performance of biobased epoxies and retard crack growth, opening new horizons for their use in structural applications and the use of these bio-inspired overlapping curls to control crack growth in adhesively bonded joints.

## 1. Introduction

Climate change is a major global issue that impacts both the environment and human society, requiring an immediate effort in enhancing sustainability in the aerospace industry. Using adhesive bonding in lightweight composites structures is a rising state-of-the-art technique for more efficient, sustainable, and lightweight aircraft. However, conventional adhesive materials are petroleum-based epoxy resins, contributing to the growing environmental, healthy, and economic concerns due to the harmful industrial processes and finite petrochemical resources. The green transition is essential for positioning bio-based adhesive materials as attracting options for integration into load-bearing structures. To enhance sustainability and concurrently uphold joint safety and reliability, there is a compelling need to improve the mechanical properties of adhesively bonded composite joints using the bio-based epoxy adhesive.

Several methods have been investigated to improve the fracture resistance of adhesively bonded joints by introducing crack arrest features, such as the corrugated substrate [1], z-pins [2], and co-cured thermoplastic barrier [3]. Another promising pathway is to architect the adhesive layer and rely on the extrinsic bridging phenomena. The adhesive layer can be directly utilized to bridge the separating CFRP parts, triggered by the patterning of distinct surface treatments [4]. Moreover, integrating lightweight inserts within the adhesive layer could further achieve progressive failure of bonded joints. The polymer carrier within the adhesive film, originally aiming for maintaining the bondline thickness, has been proven to largely enhance the energy release rate (ERR) and successfully arrest the crack propagation [5]. Following this trend, polyamide structures (individual straight wire [6] and woven 2D net [7]) were

integrated into double cantilever beams (DCBs) to improve joint fracture resistance [6, 7]. However, as already discussed by Tao et al. [6], such enhancement mainly came from the failure transition from adhesive failure to partial cohesive failure. Therefore, the fracture toughness of the used epoxy material contributed a large portion to the ultimate fracture energy, decreasing the improving significance when compared to the cohesive failure of the joints. Furthermore, the insert structures were either limited to maintaining long-range bridging [6] or difficult to trigger effective bridging [6,7], requiring a more advanced design to trigger and control the extrinsic large-scale bridging.

In this work, an extrinsic toughening mechanism under the mode I fracture loading of adhesive joints was developed, focusing on the biomimetic design of polymer microstructures integrated within a bio-based epoxy adhesive. By mimicking the molecular structure of spider silk, which is one of the toughest materials in nature, polyamide coiling fibers with sacrificial bonds and hidden lengths were manufactured through 3D printing. Such 3D-printed bio-mimic reinforcements, or overlapping curls (OCs), were integrated within a bio-based epoxy adhesive. The adhesive layer of DCB was architected to trigger the extrinsic bridging, promote progressive failure, and improve the mode I ERR. The printing and manufacturing parameters were tuned to affect the failure responses of overlapping curls, thus architecting their ability to arrest crack propagation within the integrated bio-based adhesive layer.

## 2. Materials and methods

### 2.1. Materials

Bonding substrates were [0]<sub>s</sub> carbon fiber reinforced polymers (CFRPs), made through manual stacking of unidirectional prepregs (HexPly 8552/AS4, Hexcel, USA). The substrates were cured following the supplier's recommendation in the autoclave, which consisted of a 2°C/min heating up to 110°C, holding at 110°C for 60 mins, 2°C/min heating to 180°C, 120-mins holding at 180°C, and 2°C/min cooling till 20°C. Cured plates had a nominal thickness of 1 mm and they were then cut into slices in dimension of 200 mm x 25 mm for manufacturing DCB samples. A proper surface treatment was applied to ensure cohesive failure of adhesive joints. The surfaces were first sanded by #400 sandpaper to create proper surface roughness. After being wiped with acetone, substrate surfaces were treated with UV/ozone for 7 mins to activate the surface before bonding.

Biomimetic overlapping curls were 3D printed through honey-like liquid rope coiling by adjusting the extrusion and printing speed ratio of a fused filament fabrication printer (Prusa i3 MK3S+, Prusa Research, Czech Republic), as shown in Fig. 1 (a). With a nozzle temperature of 275°C, printing bed temperature of 80°C, extrusion of 60 mm/min, and printing speed of 1000 mm/min, polyamide 6 (F3 PA Pure Pro, FiberThree, Germany) coiling fibers with sacrificial bonds and hidden length were obtained.

To bond cured CFRP substrates, GreenCast 160 bio-based epoxy resin (Sicomina, France) was adopted in this work for the adhesive material. GreenCast 160 was mixed with the hardener SD 7160 at a weight ratio of 100:42, and then the mixture was degassed under vacuum for 30 mins. To architect the adhesion patterning of DCB samples, Teflon tapes were alternatively patterned on two parallel polyamide OCs, with a spacing of 9 mm, as shown in Fig. 1 (b), to guide the cohesive crack propagation within the bondline. The degassed adhesive mixture was first poured onto one of CFRP surfaces. After placing the OCs on top of the liquid adhesive, another layer of adhesive mixture was applied, completing the entire bondline to the nominal thickness of 1 mm. At last, the other mating CFRP substrate was gently pressed to the bondline under mechanical pressure, to ensure contact at CFRP/bondline interfaces. The bonded DCB samples were kept in the room condition (22°C and 42% relative humidity) for 14 days before mode I tests.

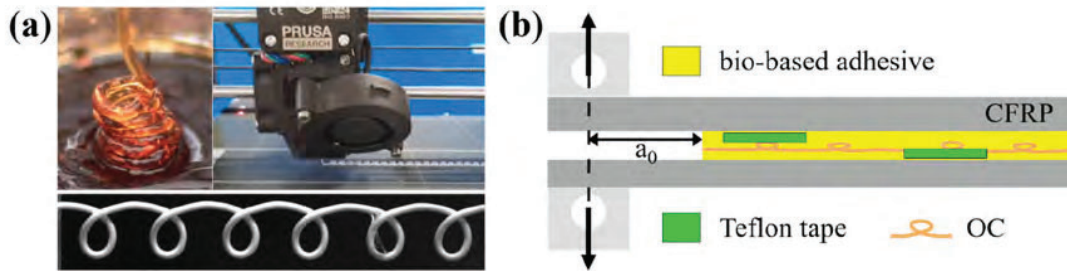


**Figure 1.** (a) 3D print polyamide overlapping curls consisting of coiling fibers with sacrificial bonds and hidden length through honey-like liquid rope coiling. (b) Schematic of DCB setup for mode I fracture characterization of overlapping curls integrated bio-based adhesive.

## 2.2. Mode I fracture tests

Quasi-static DCB tests were carried out to evaluate the mode I ERR of adhesive joints using a universal testing machine (Zwick 10kN loading frame, ZwickRoell, Netherlands) with a 1 kN load cell. A pre-crack was generated through a 50-mm long Teflon tape at the beginning of one of CFRP surfaces, leading to  $a_0=35$  mm. 1-mm spacers were used to control the bondline thickness of DCB samples. To highlight the crack advance, one side of DCB samples was painted white, and a ruler was drawn manually with a resolution of 1 mm. DCB testing was performed under 4 mm/min displacement control, following ASTM D5528-13 standard. Four DCB samples with pure GreenCast bondline and four DCB samples with OC-integrated bondline were fractured. During the tests, the crack advance was recorded by a fixed camera from the ruler side of DCB samples. A traveling microscope was mounted on the other side of DCB samples to closely visualize the crack front morphology. Both cameras captured images automatically every four seconds. Mode I ERR was obtained following the compliance calibration data reduction method:

$$G_I = \frac{nP\delta}{2ba} \quad (1)$$

where  $n$  is the calibration coefficient through fitting of  $\log(P/\delta)$ - $\log(a)$ ,  $P$  is the load,  $\delta$  is the extension,  $b$  is DCB width, and  $a$  is the crack advance distance.

## 3. Results and discussions

Typical DCB results of pure GreenCast bondline and OC-integrated bondline are highlighted in Fig. 2. Stick-slip behavior is presented in pure GreenCast bondline (red dashed line in Fig. 2 (a)), and its mode I ERR stabilized at the level of  $0.4 \text{ kJ/m}^2$ . Fracture surface observation of pure GreenCast bondline is also shown in the insert of load-displacement. Cohesive failure is present, proven by the GreenCast adhesive residue layers on both CFRP substrates. Besides, parabolic textures are shown on fractured epoxy surfaces, corresponding to the stick locations in the load-displacement curve.

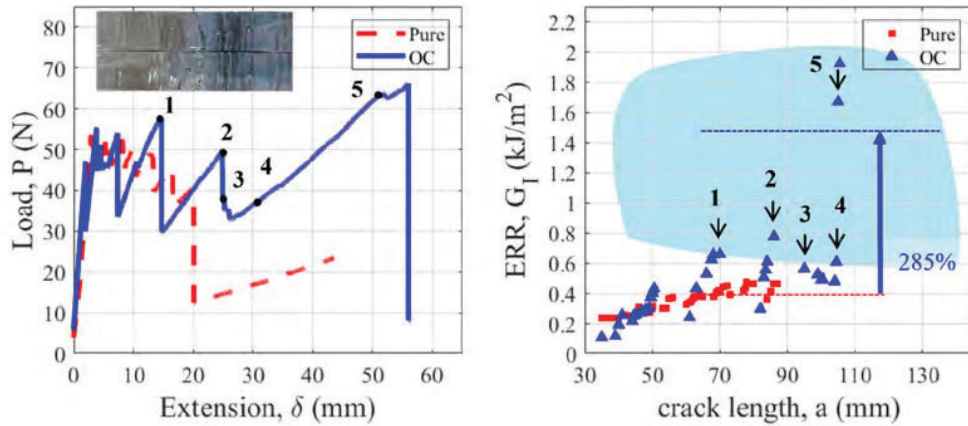


**Figure 2.** Load-displacement and mode I ERR curves of DCB samples with pure GreenCast bondline and OC-integrated bondline. The insert in the load-displacement curve is the fracture surface of the DCB sample with pure GreenCast bondline.

While DCB with OC-integrated bondline exhibits larger fluctuation in both curves. The large fluctuation occurs at a lower frequency compared to the stick-slip phenomena of pure GreenCast bondline. Five analysis points are chosen to correspond between load-displacement and ERR curves. Points 1 and 2 show local peak load values, and corresponding mode I ERR almost doubles that obtained in pure GreenCast bondline. At point 5, load increases greatly up to 15% higher than the initial peak load at 50-mm DCB arm opening, and mode I ERR was enhanced more than four times compared to the pure GreenCast bondline cohesive failure, exhibiting an incredible crack arresting feature in adhesive joints.

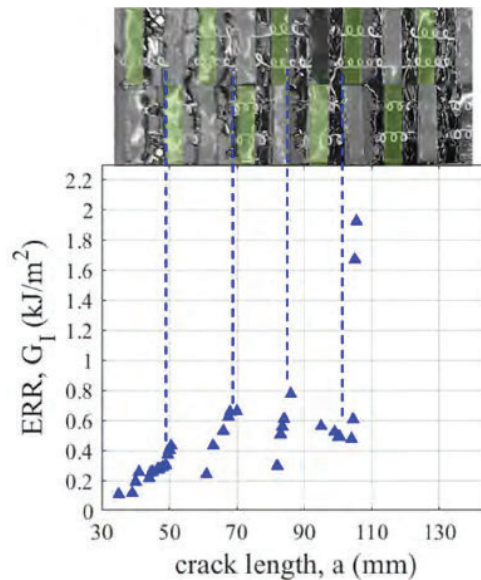


**Figure 3.** Fracture surface observation of DCB samples with OC-integrated bondline. The horizontal location of the fracture surface corresponds to the crack length distance in the x-axis. Green regions highlight Teflon tape locations patterned on OC, while blue dashed lines highlight correlations between ERR values and Teflon patterning.

Fracture surface observation of the DCB sample with OC-integrated bondline is shown in Fig. 3, together with corresponding mode I ERR values at locations on the fracture surface. Patterning of Teflon tapes is clearly presented on the fracture surface, which successfully guides the growth of crack path oscillating between two CFRP/bondline interfaces. Four blue dashed lines highlight the beginning of

the Teflon tape, which are also locations of the crack transiting to the other CFRP/bondline interface. The first three lines correlate well with the peak ERR values, showing that the crack transition is more responsible for the ERR enhancement. While the last line mismatches with the ERR increase, indicating extra toughening mechanisms.

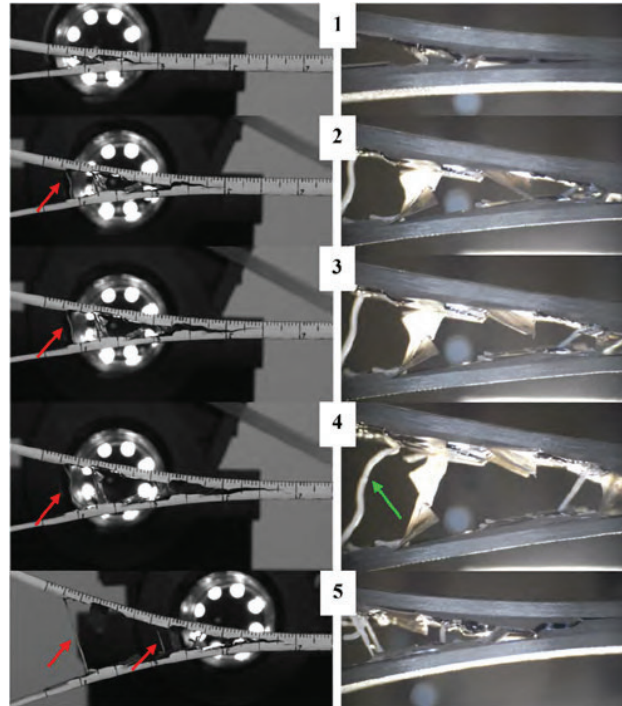


**Figure 4.** Crack advance (left) and local crack front morphology (right) observations at marked locations in both load-displacement and ERR curves of DCB sample with OC-integrated bondline. Red arrows highlight the OC bridging, while the green arrow points to the local failure of OC.

To better understand the failure mechanisms coming from the integrated overlapping curls under mode I DCB tests, five in situ observations of the crack propagation are illustrated in Fig. 4, at the corresponding points shown in Fig. 2. The left column of images was captured by the fixing crack advance camera, while the right column was taken through the traveling microscope. Crack advance observations confirm the crack path oscillation, which is from the adhesion patterning, as discussed in Fig. 3. Several bridging coiling fibers are triggered during the crack propagation and crack path oscillation. Crack advance images highlight two major bridging of overlapping curls, while a traveling microscope reveals more localized bridging OCs. Local bridging curls failed to unravel to release the hidden length of the structure, leading to early failure and limited toughening contribution. This limited exposure of coiling fibers came from the short distance (5 mm) between the Teflon tapes, eliminating the extension loaded on coiling fibers. Besides, the traveling microscope clearly illustrates the stretching, unraveling, and ultimate failure of one bridging overlapping curl, as shown in 2, 3, and 4 points in Fig. 4. At point 5, two major bridging OCs are strengthened, as highlighted by red arrows in Fig. 4. Together with multiple local bridging curls, extensive bridging phenomena can be identified at point 5, which acts as the major toughening mechanism for the large enhancement in ERR. Also, such an extrinsic bridging toughening explains the mismatch between the ERR increase and the beginning of patterned Teflon tape, as illustrated by the last blue dashed line in Fig. 3.

#### 4. Conclusions

This work investigated the toughening effect of biomimetic overlapping curls consisting of coiling fibers with sacrificial bonds and hidden length in mode I fracture of adhesively bonded CFRP joints using the

biobased GreenCast epoxy adhesive material. Biomimetic reinforcement coiling fibers were 3D printed, then patterned, and finally integrated within the GreenCast bondline. DCB results showed an increase of 285% in mode I ERR thanks to the crack path oscillation and extrinsic bridging. It has been shown that triggered bridging of biomimetic overlapping curls successfully arrests crack propagation, and the hidden length of coiling fibers allows for extended bridging of separating DCB arms, paving a novel path towards safer and more sustainable aerospace structures.

### Acknowledgments

The authors acknowledge Fundação para a Ciência e a Tecnologia (FCT) for its financial support via the project LAETA Base Funding (DOI: 10.54499/UIDB/50022/2020).

### References

- [1] K. I. Tserpes, G. Peikert, I. S. Floros. Crack stopping in composite adhesively bonded joints through corrugation. *Theoretical and Applied Fracture Mechanics* 83: 152–7, 2016.
- [2] J. Hoffmann, G. Scharr. Mode I delamination fatigue resistance of unidirectional and quasi-isotropic composite laminates reinforced with rectangular z-pins. *Composites Part A: Applied Science and Manufacturing* 115: 228–35, 2018.
- [3] T. Löbel, D. Holzhüter, M. Sinapius M, C. Hühne. A hybrid bondline concept for bonded composite joints. *International Journal of Adhesion and Adhesives* 68: 229–38, 2016.
- [4] R. Tao, X. Li, A. Yudhanto, M. Alfano, and G. Lubineau. Laser-based interfacial patterning enables toughening of CFRP/epoxy joints through bridging of adhesive ligaments. *Composites Part A: Applied Science and Manufacturing* 139: 106094, 2020.
- [5] S. Heide-Jørgensen, S. Teixeira de Freitas, and M. K. Budzik. On the fracture behaviour of CFRP bonded joints under mode I loading: Effect of supporting carrier and interface contamination. *Composites Science and Technology* 160: 97-110, 2018.
- [6] A. Yudhanto, M. Almulhim, F. Kamal, R. Tao, L. Fatta, M. Alfano, G. Lubineau. Enhancement of fracture toughness in secondary bonded CFRP using hybrid thermoplastic/thermoset bondline architecture. *Composites Science and Technology* 199: 108346, 2020.
- [7] R. Tao, X. Li, A. Yudhanto, M. Alfano, G. Lubineau. Toughening adhesive joints through crack path engineering using integrated polyamide wires. *Composites Part A: Applied Science and Manufacturing* 158: 106954, 2022.